



**ARTICLE**

## Finite Element Analysis of the Electromagnetics of Continuum

Shuaiqi Song, Lijie Grace Zhang and James D. Lee\*

Department of Mechanical and Aerospace Engineering, The George Washington University, Washington, DC, USA

\*Corresponding Author: James D. Lee. Email: [jdlee@gwu.edu](mailto:jdlee@gwu.edu)

Received: 12 February 2026; Accepted: 27 April 2026; Published: 30 June 2026

**ABSTRACT:** The theory of thermomechanical-electromagnetic coupling was constructed. The finite element analysis of thermo-visco-elastic-plastic-electromagnetic continuum was formulated. Then the problem of wave propagation in this continuum was solved in two stages. In Stage I, a nearly static thermomechanical solution of a hollow cylinder, subject to twist and temperature gradient, was obtained. Then, in Stage II, the problem of wave propagation of scalar and vector potentials, due to deformation and temperature gradient, was solved. In the second approach, in Stage I, the static electric field and static magnetic field are obtained through static scalar and vector potentials, then in Stage II, the dynamic solutions of temperature, plastic strains, von Mises stress, and current were solved.

**KEYWORDS:** Electromagnetics of continuum; finite element formulation; constitutive theory; thermo-visco-elastic-plastic-electromagnetic material; geometrically nonlinear; scalar and vector potentials

### 1 Introduction

Electromagnetics of Continuum is defined as a branch of the physical sciences concerned with the interaction of electromagnetic fields with a deformable body. The ultimate goal of this work is to formulate the finite element equations for an electromagnetic continuum. To begin with, notice that the balance laws of electromagnetics continuum consist of two parts: the thermomechanical (TM) part and the electromagnetic (EM) part. The work can be applied to more complex substances, so it can be utilized to treat electrodynamic-related composite materials. Incorporating the coupling between thermomechanics and electromagnetics into a unified theory can further enhance understanding and prediction of large classes of physical phenomena and provide many technological applications. Phenomenologically important cross effects, such as Peltier, Seebeck, Hall, Ettingshausen, Righi-Leduc, and Nernst effects, can now be studied theoretically and numerically.

The electromagnetic (EM) balance laws, i.e., the famous Maxwell's equations, are introduced. We also introduce the Lorentz Transformation of  $\mathbf{E}$  and  $\mathbf{B}$  fields in relativistic electromagnetic theory [1], as well as in its special case, non-relativistic electromagnetic theory.

Then the Eulerian description of the basic laws of continuum theory, i.e., *Conservation of Mass*, *Balance of Linear Momentum*, *Balance of Angular Momentum*, *Conservation of Energy*, and *Entropy Principle*, is introduced. Also included in these basic laws are the electromagnetic (EM) part of the body force, body moment, and energy source [2–6]. It is emphasized that this inclusion establishes the link between the thermomechanical part (TM) and the electromagnetic part (EM) of the electrodynamics of continuum.

Then we formulated the constitutive theory for thermo-visco-elastic-plastic-electromagnetic (TVEP-TM) materials. The formulation of constitutive theory, including plasticity, is unique in the sense that one needs to add a set of internal variables to the list of independent constitutive variables and, of course, one needs to supply a set of governing equations for the newly added internal variables [7]. Following that, we specialized the materially linear constitutive equations. It is emphasized that this work is based on *geometrically nonlinear*, or say large-strain, approaches. *Onsager's postulate* is utilized for the derivation of viscosity. *Return-Mapping-Algorithm* is invoked for plasticity.

It is a well-known physical fact that the electric field  $\mathbf{E}$  and the magnetic flux  $\mathbf{B}$  are not independent from each other, nor are the dielectric displacement  $\mathbf{D}$  and the magnetic field  $\mathbf{H}$ . To resolve this problem, especially for the finite element formulation, the scalar potential  $\phi$  and the vector potential  $\mathbf{A}$  are introduced [1], which are related to the electric field  $\mathbf{E}$  and magnetic flux  $\mathbf{B}$  as

$$\mathbf{B} \equiv \nabla \times \mathbf{A}, \quad \mathbf{E} \equiv -\nabla \phi - \frac{1}{c} \frac{\partial \mathbf{A}}{\partial t}$$

Eventually, the governing equations for  $\phi$  and  $\mathbf{A}$ , not  $\mathbf{E}$  and  $\mathbf{B}$ , are obtained in [Section 6](#).

For the finite element formulation, we link the displacement  $\mathbf{U}$ , temperature  $\mathbf{T}$ , scalar potential  $\phi$ , and vector potential  $\mathbf{A}$  at a generic point in a finite element to the corresponding nodal values associated with that finite element. Finally, the finite element equations for  $U_{K\beta}$ ,  $T_\beta$ ,  $\phi_\beta$ , and  $A_{k\beta}$  are obtained. It is proposed to solve a torsion problem of a cylinder in two approaches, each of which has two stages. The results will show the coupling between electromagnetics and thermomechanics.

## 2 Maxwell's Equations

The balance laws of electromagnetics of continuum consist of two parts: the thermomechanical (TM) part and the electromagnetic (EM) part. The EM balance laws are the well-known Maxwell's equations that can be expressed in the Heaviside-Lorentz system [1,5,6] as

$$\nabla \cdot \mathbf{D} = q \quad \text{or} \quad D_{k,k} = q \tag{1}$$

$$\nabla \times \mathbf{E} + \frac{1}{c} \frac{\partial \mathbf{B}}{\partial t} = 0 \quad \text{or} \quad e_{ijk} E_{k,j} + \frac{1}{c} \frac{\partial B_i}{\partial t} = 0 \tag{2}$$

$$\nabla \cdot \mathbf{B} = 0 \quad \text{or} \quad B_{k,k} = 0 \tag{3}$$

$$\nabla \times \mathbf{H} - \frac{1}{c} \frac{\partial \mathbf{D}}{\partial t} = \frac{1}{c} \mathbf{J} \quad \text{or} \quad e_{ijk} H_{k,j} - \frac{1}{c} \frac{\partial D_i}{\partial t} = \frac{1}{c} J_i \tag{4}$$

where  $\mathbf{D}$  is the dielectric displacement vector,  $\mathbf{B}$  the magnetic induction vector,  $\mathbf{E}$  the electric field vector,  $\mathbf{H}$  the magnetic field vector,  $\mathbf{J}$  the total current vector, and  $q$  the free charge density.

Define the polarization vector  $\mathbf{P}$  and the magnetization vector  $\mathbf{M}$  as

$$\begin{aligned} \mathbf{P} &= \mathbf{D} - \mathbf{E} \quad \text{or} \quad P_k = D_k - E_k \\ \mathbf{M} &= \mathbf{B} - \mathbf{H} \quad \text{or} \quad M_k = B_k - H_k \end{aligned} \tag{5}$$

It is noticed that the quantities  $q, \mathbf{J}, \mathbf{D}, \mathbf{E}, \mathbf{P}, \mathbf{B}, \mathbf{H}, \mathbf{M}$  are all referred to a fixed laboratory frame  $R_G$ . On the other hand,  $q^*, \mathbf{J}^*, \mathbf{D}^*, \mathbf{E}^*, \mathbf{P}^*, \mathbf{B}^*, \mathbf{H}^*, \mathbf{M}^*$  are referred to a co-moving reference frame  $R_C$ .

In relativistic electromagnetic theory, the Lorentz Transformation of  $\mathbf{E}$  and  $\mathbf{B}$  fields can be expressed as [1]

$$\mathbf{E}^* = \gamma (\mathbf{E} + \boldsymbol{\beta} \times \mathbf{B}) - \frac{\gamma^2}{\gamma + 1} \boldsymbol{\beta} (\boldsymbol{\beta} \cdot \mathbf{E}) \quad (6)$$

$$\mathbf{B}^* = \gamma (\mathbf{B} - \boldsymbol{\beta} \times \mathbf{E}) - \frac{\gamma^2}{\gamma + 1} \boldsymbol{\beta} (\boldsymbol{\beta} \cdot \mathbf{B}) \quad (7)$$

where  $\boldsymbol{\beta} \equiv \frac{\mathbf{v}}{c}$ ,  $\beta = \sqrt{\boldsymbol{\beta} \cdot \boldsymbol{\beta}}$ ,  $\gamma \equiv \frac{1}{\sqrt{1-\beta^2}}$ , and  $\mathbf{v}$  is the velocity of the co-moving frame  $R_C$  relative to the fixed laboratory frame  $R_G$ , and  $c$  is the speed of light in vacuum. Jackson also explained that the inverse can be found by interchanging the star and the no-star quantities and by changing  $\boldsymbol{\beta}$  to  $-\boldsymbol{\beta}$ , i.e.,

$$\mathbf{E} = \gamma (\mathbf{E}^* - \boldsymbol{\beta} \times \mathbf{B}^*) - \frac{\gamma^2}{\gamma + 1} \boldsymbol{\beta} (\boldsymbol{\beta} \cdot \mathbf{E}^*) \quad (8)$$

$$\mathbf{B} = \gamma (\mathbf{B}^* + \boldsymbol{\beta} \times \mathbf{E}^*) - \frac{\gamma^2}{\gamma + 1} \boldsymbol{\beta} (\boldsymbol{\beta} \cdot \mathbf{B}^*) \quad (9)$$

Recall that  $\gamma \equiv (1 - \beta^2)^{-\frac{1}{2}}$ , the Taylor series expansion of  $\gamma$  about  $\beta = 0$  is obtained as

$$\gamma \approx 1 + \frac{1}{2}\beta^2 + \frac{3}{4}\beta^4 + \dots \quad (10)$$

Let's keep the Taylor series at most to  $\beta^2$ . Then, for non-relativistic electromagnetic theory, we have

$$\mathbf{E}^* = \mathbf{E} + \boldsymbol{\beta} \times \mathbf{B}, \quad \mathbf{E} = \mathbf{E}^* - \boldsymbol{\beta} \times \mathbf{B}^* \quad (11)$$

$$\mathbf{B}^* = \mathbf{B} - \boldsymbol{\beta} \times \mathbf{E}, \quad \mathbf{B} = \mathbf{B}^* + \boldsymbol{\beta} \times \mathbf{E}^* \quad (12)$$

$$\mathbf{D}^* = \mathbf{D} + \boldsymbol{\beta} \times \mathbf{H}, \quad \mathbf{D} = \mathbf{D}^* - \boldsymbol{\beta} \times \mathbf{H}^* \quad (13)$$

$$\mathbf{H}^* = \mathbf{H} - \boldsymbol{\beta} \times \mathbf{D}, \quad \mathbf{H} = \mathbf{H}^* + \boldsymbol{\beta} \times \mathbf{D}^* \quad (14)$$

$$\mathbf{P}^* = \mathbf{P} - \boldsymbol{\beta} \times \mathbf{M}, \quad \mathbf{P} = \mathbf{P}^* + \boldsymbol{\beta} \times \mathbf{M}^* \quad (15)$$

$$\mathbf{M}^* = \mathbf{M} + \boldsymbol{\beta} \times \mathbf{P}, \quad \mathbf{M} = \mathbf{M}^* - \boldsymbol{\beta} \times \mathbf{P}^* \quad (16)$$

Also, it is noticed that Eringen [3] gave a detailed discussion and derivation, and showed that

$$q^* = q, \quad \mathbf{J}^* = \mathbf{J} - q\mathbf{v} \quad (17)$$

### 3 Balance Laws of Continuum Theory

The Eulerian description of the basic laws of continuum theory can be expressed as [4]:

*Conservation of Mass*

$$\dot{\rho} + \rho v_{k,k} = 0 \quad (18)$$

*Balance of Linear Momentum*

$$t_{ji,j} + \rho (f_i - \dot{v}_i) + F_i = 0 \quad (19)$$

*Balance of Angular Momentum*

$$\varepsilon_{kij}t_{ij} + C_k = 0 \quad (20)$$

*Conservation of Energy*

$$\rho \dot{e} - t_{kl}v_{l,k} + q_{k,k} - \rho h - W = 0 \quad (21)$$

*Entropy Principle (Second Law of Thermodynamics)*

$$\rho \dot{\eta} + \left( \frac{q_i}{\theta} \right)_{,i} - \frac{\rho h}{\theta} \geq 0 \quad (22)$$

where  $\rho$ ,  $t_{kl} \neq t_{lk}$ ,  $e$ ,  $q_k$ ,  $\eta$ ,  $\theta$ ,  $v_i$ ,  $f_i$ ,  $F_i$ ,  $C_k$ ,  $h$ , and  $W$  are the mass density, Cauchy stress, internal energy density, heat flux, entropy density, absolute temperature, velocity, body force (TM), body force (EM), body moment (EM), energy source (TM), and energy source (EM), respectively.

The EM part of the body force, body moment, and energy source are given as [2-6]:

$$F_k = qE_k + E_{l,k}P_l + B_{l,k}M_l + \frac{1}{c}e_{klm} \left\{ J_l B_m + (v_n P_l B_m)_{,n} + \frac{\partial}{\partial t} (P_l B_m) \right\} \quad (23)$$

$$C_k = \varepsilon_{ijk} \{ P_i E_j^* + M_i^* B_j \} \quad (24)$$

$$W = E_k^* (\dot{P}_k + P_k v_{l,l}) - M_k^* \dot{B}_k + J_k^* E_k^* \quad (25)$$

Notice that, if  $A$  is a function of the Eulerian coordinate  $x_i$  and time  $t$ , then  $\dot{A} = \frac{\partial A}{\partial t} + A_{,i}v_i$ .

Let the Helmholtz free energy density in this work be defined as

$$\psi \equiv e - \theta \eta - \rho^{-1} E_k^* P_k \quad (26)$$

Notice that this expression of Helmholtz free energy density is different from that in classical continuum mechanics, i.e., the inclusion of  $-\rho^{-1} E_k^* P_k$ . However, the expression of Helmholtz free energy density is the same as that in micromorphic theory [8]. In other words, the expression of the Helmholtz free energy density is hinged on whether the work has thermomechanical and electromagnetic coupling. Classical continuum mechanics and microcontinuum theory [4] (including micromorphic theory) are two completely different theories, and yet they have many essentials and fundamental principles in common. Therefore, in order to reduce overlap, interested readers are recommended to read [8].

Then one obtains the Lagrangian description of the law of conservation of energy and the Clausius-Duhem (CD) inequality as [7]

$$\rho^o \dot{e} = T_{KL}^m \dot{E}_{KL} - Q_{K,K} - P_K \dot{E}_K^* - M_K^* \dot{B}_K + J_K^* E_K^* - \rho^o h \quad (27)$$

$$- \rho^o (\dot{\psi} + \eta \dot{\theta}) + T_{KL}^m \dot{E}_{KL} - \frac{1}{\theta} Q_K \theta_{,K} - P_K \dot{E}_K^* - M_K^* \dot{B}_K + J_K^* E_K^* \geq 0 \quad (28)$$

where the mechanical part of the Cauchy stress,  $t_{kl}^m$  is defined as

$$t_{kl}^m \equiv t_{kl} - t_{kl}^{em}, \quad T_{KL}^m \equiv J t_{kl}^m X_{K,k} X_{L,l} \quad (29)$$

And the electromagnetic part of the Cauchy stress,  $t_{kl}^{em}$  is defined as

$$t_{kl}^{em} \equiv -P_k E_l^* - M_k^* B_l \quad (30)$$

Now one may verify that

$$\begin{aligned} \varepsilon_{ikl} t_{kl}^m &= \varepsilon_{ikl} \{t_{kl} - t_{kl}^{em}\} \\ &= \varepsilon_{ikl} \{t_{kl} + P_k E_l^* + M_k^* B_l\} \\ &= \varepsilon_{ikl} \{t_{kl} + C_i\} \quad \Leftarrow \text{Eq. (30)} \\ &= 0 \quad \Leftarrow \text{Eq. (20)} \end{aligned} \quad (31)$$

which implies the symmetry of the mechanical part of the Cauchy stress tensor, i.e.,

$$t_{kl}^m = t_{lk}^m, \quad T_{KL}^m = T_{LK}^m \quad (32)$$

Notice that  $t_{kl} \neq t_{lk}$ ,  $t_{kl}^{em} \neq t_{lk}^{em}$ . If there is no coupling with electromagnetics, i.e.,  $\mathbf{P} = \mathbf{E}^* = 0$ , and  $\mathbf{M}^* = \mathbf{B} = 0$ , then one has

$$t_{kl}^m = t_{kl}, \quad t_{kl}^{em} = 0 \quad (33)$$

#### 4 Constitutive Equations

In this section, we are going to formulate the constitutive theory for thermo-visco-elastic-plastic-electromagnetic (TVEP-TM) materials. The formulation of constitutive theory, including plasticity, is unique in the sense that one needs to add a set of internal variables to the list of independent constitutive variables and, of course, one needs to supply a set of governing equations for the newly added internal variables [9]. For the electrodynamics of a continuum, a set of internal variables is introduced as [7]

$$\mathbf{W} = \{\mathbf{E}^p, \mathbf{R}\} \quad (34)$$

where  $\mathbf{E}^p$  is the plastic strain corresponding to the Lagrangian strain  $\mathbf{E}$  defined as

$$E_{KL} \equiv \frac{1}{2} (x_{k,K} x_{k,L} - \delta_{KL}) \quad (35)$$

And  $\mathbf{R}$ , named as the hardening parameters, is a generalized vector of internal variables.

Now, let the formulation of the constitutive theory for the TVEP-EM materials begin with

$$\mathbf{Z} = \mathbf{Z}(\mathbf{Y}) \quad (36)$$

where

$$\mathbf{Z} = \{\mathbf{T}^m, \mathbf{Q}, \psi, \eta, \mathbf{P}, \mathbf{M}^*, \mathbf{J}^*\} = \{T_{KL}^m, Q_K, \psi, \eta, P_K, M_K^*, J_K^*\} \quad (37)$$

$$\mathbf{Y} = \{\mathbf{E}, \dot{\mathbf{E}}, \theta, \nabla\theta, \mathbf{E}^*, \mathbf{B}, \mathbf{E}^p, \mathbf{R}\} \quad (38)$$

The definitions of  $T_{KL}^m$ ,  $T_{KL}$ ,  $Q_K$ ,  $E_K^*$ ,  $B_K$ ,  $P_K$ ,  $M_K^*$ , and  $J_K^*$  are given as

$$\begin{aligned} T_{KL}^m &\equiv J t_{kl}^m X_{K,k} X_{L,l}, \quad T_{KL} \equiv J t_{kl} X_{K,k} X_{L,l}, \quad Q_K \equiv J q_k X_{K,k} \\ P_K &\equiv J P_k X_{K,k}, \quad M_K^* \equiv J M_k^* X_{K,k}, \quad J_K^* \equiv J J_k^* X_{K,k} \end{aligned} \quad (39)$$

$$E_K^* \equiv E_k^* x_{k,K}, \quad B_K \equiv B_k x_{k,K}$$

Following the same procedures in [8], a scalar-valued yield function is defined as

$$f = f(\mathbf{Y}) \quad (40)$$

For a set of fixed values of  $\mathbf{W}$ , a hyper surface, named the yield surface, is determined by

$$f(\mathbf{Y}) = 0 \quad (41)$$

Define the loading rate  $\lambda$  as the scalar product between the outward normal to the yield surface and the tangent vector to the trajectory of  $\mathbf{E}$ ,  $\dot{\mathbf{E}}$ ,  $\theta$ ,  $\nabla\theta$ ,  $\mathbf{E}^*$ ,  $\mathbf{B}$ , i.e.,

$$\lambda = \frac{\partial f}{\partial E_{KL}} \dot{E}_{KL} + \frac{\partial f}{\partial \theta} \dot{\theta} + \frac{\partial f}{\partial \dot{E}_{KL}} \ddot{E}_{KL} + \frac{\partial f}{\partial \theta_{,K}} \dot{\theta}_{,K} + \frac{\partial f}{\partial E_K^*} \dot{E}_K^* + \frac{\partial f}{\partial B_K} \dot{B}_K \quad (42)$$

Three distinct cases, unloading, neutral loading, and loading, are defined as: (a)  $f < 0$ , (b)  $f = \lambda = 0$ , and (c)  $f = 0$ ,  $\lambda > 0$ , respectively. The internal variables of plasticity  $\mathbf{W}$  will remain unchanged in the cases of unloading and neutral loading. The governing equations for the internal variables of plasticity  $\mathbf{W}$  are proposed to be

$$\dot{\mathbf{W}} = \lambda^* \Phi(\mathbf{Y}) \quad (43)$$

where

$$\lambda^* = \begin{cases} 0 & \text{if } f < 0 \quad \text{or} \quad \lambda < 0 \\ \lambda & \text{if } f = 0 \quad \text{and} \quad \lambda \geq 0 \end{cases} \quad (44)$$

Now we substitute Eqs. (36) and (42) into the Clausius-Duhem inequality, Eq. (28). It leads to

$$-\rho^o \left\{ \frac{\partial \psi}{\partial E_{KL}} \dot{E}_{KL} + \frac{\partial \psi}{\partial \dot{E}_{KL}} \ddot{E}_{KL} + \frac{\partial \psi}{\partial \theta} \dot{\theta} + \frac{\partial \psi}{\partial \theta_{,K}} \dot{\theta}_{,K} + \frac{\partial \psi}{\partial E_K^*} \dot{E}_K^* + \frac{\partial \psi}{\partial B_K} \dot{B}_K + \eta \dot{\theta} + \frac{\partial \psi}{\partial \mathbf{W}} \cdot \lambda^* \Phi \right\} + T_{KL}^m \dot{E}_{KL} - \frac{1}{\theta} Q_K \theta_{,K} - P_K \dot{E}_K^* - M_K^* \dot{B}_K + J_K^* E_K^* \geq 0 \quad (45)$$

Since this inequality is linear in  $\ddot{E}_{KL}$ ,  $\dot{E}_K^*$ ,  $\dot{B}_K$ ,  $\dot{\theta}$ ,  $\dot{\theta}_{,K}$ , it leads to

$$\psi = \psi(E_{KL}, \theta, E_K^*, B_K, E_{KL}^p, \mathbf{R}) \quad (46)$$

$$\eta = -\frac{\partial \psi}{\partial \theta} \quad (47)$$

$$T_{KL}^m \equiv \rho^o \frac{\partial \psi}{\partial E_{KL}}, \quad T_{KL}^m = T_{KL}^{me} + T_{KL}^{md}(\mathbf{Y}) \quad (48)$$

$$P_K = -\rho^o \frac{\partial \psi}{\partial E_K^*} \quad (49)$$

$$M_K^* = -\rho^o \frac{\partial \psi}{\partial B_K} \quad (50)$$

$$T_{KL}^{md} \dot{E}_{KL} - \frac{1}{\theta} Q_K \theta_{,K} + J_K^* E_K^* - \rho^o \frac{\partial \psi}{\partial \mathbf{W}} \cdot \lambda^* \Phi \geq 0 \quad (51)$$

where the superscript  $d$  refers to the dissipative part and superscript  $e$  refers to the elastic part, or say, the reversible part. Since the inequality, Eq. (51), must be satisfied for any value of the loading rate  $\lambda$ , it implies

$$\frac{\partial \psi}{\partial \mathbf{W}} \cdot \Phi \leq 0 \quad (52)$$

$$T_{KL}^{md} \dot{E}_{KL} - \frac{1}{\theta} Q_K \theta_{,K} + J_K^* E_K^* \geq 0 \quad (53)$$

Also, it should be emphasized that, in the case of loading, a TVEP-EM state leads to another TVEP-EM state. In other words, the consistency condition of plasticity requires that  $f = 0$  and  $\lambda > 0$  lead to another state with  $f = 0$  [10]. Therefore, in the case of loading, we have  $\dot{f} = 0$ , i.e.,

$$\dot{f} = \lambda^* + \frac{\partial f}{\partial \mathbf{W}} \cdot \dot{\mathbf{W}} = \lambda^* + \lambda^* \frac{\partial f}{\partial \mathbf{W}} \cdot \Phi = \lambda^* \left( 1 + \frac{\partial f}{\partial \mathbf{W}} \cdot \Phi \right) = 0 \quad (54)$$

This gives another constitutive constraint to the plasticity

$$\frac{\partial f}{\partial \mathbf{W}} \cdot \Phi = -1 \quad (55)$$

## 5 Linear Constitutive Equations

For TVEP-EM solid, define the potential energy density function  $\Sigma$  as

$$\Sigma \equiv \rho^o \psi = \Sigma(\mathbf{E}, \theta, \mathbf{E}^*, \mathbf{B}, \mathbf{E}^p, \mathbf{R}) \quad (56)$$

Following the idea of Green and Naghdi [11], and assuming the hardening parameters  $\mathbf{R}$  do not appear in the potential energy density function, Eq. (56) can now be written as

$$\begin{aligned} \Sigma &= \Sigma(\mathbf{E} - \mathbf{E}^p, T, \mathbf{E}^*, \mathbf{B}) \equiv \Sigma(\mathbf{E}^e, T, \mathbf{E}^*, \mathbf{B}) \\ &= \Sigma^o - \rho^o \eta^o T - \frac{1}{2} \rho^o \gamma \frac{T^2}{T^o} - \bar{A}_{KL} E_{KL}^e T + a_K T E_K^* + b_K T B_K \\ &\quad + \frac{1}{2} A_{KLMN} E_{KL}^e E_{MN}^e + F_{KLM}^1 E_{KL}^e E_M^* + F_{KLM}^2 E_{KL}^e B_M \\ &\quad - \frac{1}{2} D_{KL}^1 E_K^* E_L^* - \frac{1}{2} D_{KL}^2 B_K B_L - D_{KL}^3 E_K^* B_L \end{aligned} \quad (57)$$

where  $T^o$  is the reference temperature and  $T$  is the temperature variation, and

$$T \equiv \theta - T^o, \quad T^o > 0, \quad |T| \ll T^o \quad (58)$$

From now on, we assume that the material is isotropic. Therefore, all the odd-order material property tensors are vanishing. Then it is straightforward to obtain

$$\begin{aligned} \eta &= -\frac{\partial \psi}{\partial \theta} = -\frac{\partial \psi}{\partial T} \\ &= \eta^o + \gamma \frac{T}{T^o} + \frac{\bar{A}_{KL} E_{KL}^e}{\rho^o} \end{aligned} \quad (59)$$

$$T_{KL}^{me} = \rho^o \frac{\partial \psi}{\partial E_{KL}} = \frac{\partial \Sigma}{\partial E_{KL}} = -\bar{A}_{KL} T + A_{KLMN} E_{MN}^e \quad (60)$$

$$P_K = -\rho^o \frac{\partial \psi}{\partial E_K^*} = D_{KL}^1 E_L^* + D_{KL}^3 B_L \quad (61)$$

$$M_K^* = -\rho^o \frac{\partial \psi}{\partial B_K} = D_{KL}^2 B_L + D_{LK}^3 E_L^* \quad (62)$$

Moreover, the 2nd order and 4th order material property tensors are made of a few material constants, i.e.,

$$\begin{aligned} \bar{A}_{KL} &= \bar{A} \delta_{KL}, & D_{KL}^1 &= D^1 \delta_{KL}, & D_{KL}^2 &= D^2 \delta_{KL}, & D_{KL}^3 &= D^3 \delta_{KL} \\ A_{KLMN} &= \lambda^1 \delta_{KL} \delta_{MN} + \mu^{11} \delta_{KM} \delta_{LN} + \mu^{12} \delta_{KN} \delta_{LM} \end{aligned} \quad (63)$$

### Onsager's Postulate

Now we follow Onsager's Postulate and construct a potential of dissipation quadratic as [12,13]

$$D = \frac{1}{2} d_{KLMN} \dot{E}_{KL} \dot{E}_{MN} + \frac{1}{2} g_{MN}^1 \theta_{,M} \theta_{,N} + g_{MN}^2 \theta_{,M} E_N^* + \frac{1}{2} g_{MN}^3 E_M^* E_N^* \quad (64)$$

where  $\dot{\mathbf{E}}$ ,  $\nabla \theta$ , and  $\mathbf{E}^*$  are the thermodynamic forces. Correspondingly, the thermodynamic fluxes  $\mathbf{T}^{md}$ ,  $\mathbf{Q}$ , and  $\mathbf{J}^*$  can be obtained as

$$T_{KL}^{md} = \frac{\partial D}{\partial \dot{E}_{KL}} = d_{KLMN} \dot{E}_{MN} \rightarrow d^1 \dot{E}_{MM} \delta_{KL} + 2d^2 \dot{E}_{KL} \quad (65)$$

$$-\frac{1}{\theta} Q_M = \frac{\partial D}{\partial \theta_{,M}} = g_{MN}^1 \theta_{,N} + g_{MN}^2 E_N^* \rightarrow g^1 \theta_{,M} + g^2 E_M^* \quad (66)$$

$$J_M^* = \frac{\partial D}{\partial E_M^*} = g_{NM}^2 \theta_{,N} + g_{MN}^3 E_N^* \rightarrow g^2 \theta_{,M} + g^3 E_M^* \quad (67)$$

One may verify that the CD inequality  $\mathbf{T}^{md} : \dot{\mathbf{E}} - \frac{1}{\theta} \mathbf{Q} \cdot \nabla \theta + \mathbf{J}^* \cdot \mathbf{E}^* \geq 0$  is now reduced to  $D \geq 0$ , which is precisely what the Onsager's Postulate means.

### Return Mapping Algorithm for Plasticity

Notice that  $\mathbf{E} = \mathbf{E}^e + \mathbf{E}^p$ . Now, let the hardening parameters  $\mathbf{R}$  be decomposed into two parts: the vector part  $\mathbf{G}$ , which has the same dimension as  $\mathbf{E}$ , and a scalar part  $g$ . We propose a yield function as [7]

$$f = \|\mathbf{E} - \mathbf{E}^p - \mathbf{G}\| - (E_Y + \kappa H g) = \|\mathbf{E}^e - \mathbf{G}\| - (E_Y + \kappa H g) \quad (68)$$

where  $E_Y$ ,  $H$ , and  $\kappa$  are material constants. Following the same procedures in [8], let the evolution equations for the plastic strain tensor and the hardening parameters be

$$\dot{\mathbf{E}}^p = \Omega \frac{\boldsymbol{\xi}}{\|\boldsymbol{\xi}\|}, \quad \dot{\mathbf{G}} = \Omega C_1 (1 - \kappa) H \frac{\boldsymbol{\xi}}{\|\boldsymbol{\xi}\|}, \quad \dot{g} = \Omega C_2 \quad (69)$$

where

$$\boldsymbol{\xi} \equiv \mathbf{E} - \mathbf{E}^p - \mathbf{G} = \mathbf{E}^e - \mathbf{G}, \quad \|\boldsymbol{\xi}\| \equiv \{\boldsymbol{\xi} \cdot \boldsymbol{\xi}\}^{\frac{1}{2}} \quad (70)$$

The trial value of the yield function at  $t = t_{n+1}$ , based on elastic prediction, is calculated as

$$\tilde{f}_{n+1} = \|\mathbf{E}_{n+1} - \mathbf{E}_n^p - \mathbf{G}_n\| - (E_Y + \kappa H g_n) \equiv \|\tilde{\boldsymbol{\xi}}_{n+1}\| - (E_Y + \kappa H g_n) \quad (71)$$

If  $\tilde{f}_{n+1} \leq 0$ , which means the elastic prediction is correct, then the plastic strain and hardening parameters at  $t = t_{n+1}$  maintain their values at  $t = t_n$ , i.e.,

$$f_{n+1} = \|\mathbf{E}_{n+1} - \mathbf{E}_n^p - \mathbf{G}_n\| - (E_Y + \kappa H g_n) \quad (72)$$

It is worthwhile to mention that, in this case, i.e.,  $\tilde{f}_{n+1} \leq 0$ ,  $t = t_{n+1}$ , one has  $\mathbf{E}_{n+1}^p = \mathbf{E}_n^p$ ,  $\mathbf{G}_{n+1} = \mathbf{G}_n$ , and  $g_{n+1} = g_n$ .

If  $\tilde{f}_{n+1} > 0$ , which means the elastic prediction is incorrect, then the values of plastic strain and hardening parameters at  $t = t_{n+1}$  should be updated as follows:

$$\mathbf{E}_{n+1}^p = \mathbf{E}_n^p + \Delta\Omega \tilde{\boldsymbol{\xi}}_{n+1} / \|\tilde{\boldsymbol{\xi}}_{n+1}\| \quad (73)$$

$$\mathbf{G}_{n+1} = \mathbf{G}_n + \Delta\Omega C_1 (1 - \kappa) H \tilde{\boldsymbol{\xi}}_{n+1} / \|\tilde{\boldsymbol{\xi}}_{n+1}\| \quad (74)$$

$$g_{n+1} = g_n + \Delta\Omega C_2 \quad (75)$$

where

$$\Delta\Omega = \frac{\tilde{f}_{n+1}}{1 + C_1 H - (C_1 - C_2) \kappa H} \quad (76)$$

Now, one can prove that the yield function is based on the updated  $\mathbf{E}_{n+1}^p$ ,  $\mathbf{G}_{n+1}$ ,  $g_{n+1}$  returns to zero [7] i.e.,

$$f_{n+1} = \|\mathbf{E} - \mathbf{E}_{n+1}^p - \mathbf{G}_{n+1}\| - (E_Y + \kappa H g_{n+1}) = 0 \quad (77)$$

From Eqs. (60)–(62), it is noticed that the elastic parts of the stresses,  $T_{KL}^{me}$ , and  $P_K$ , and  $M_K^*$  depend on the elastic strains, not the total strains. Using the *Return Mapping Algorithm*, one may find the plastic strains exactly, and once the total strains are found, usually through finite element analysis (to be discussed later), then immediately elastic strains and elastic parts of the stresses as well are obtained. Also, it is seen that the *Return Mapping Algorithm* is strain-based, not stress-based. Because in this formulation the stresses have two parts: elastic parts and dissipative parts, which depend on strain rates. A strain-based *Return Mapping Algorithm* works independently of strain rates.

## 6 Scalar and Vector Potentials

It is a well-known physical fact that the electric field  $\mathbf{E}$  and the magnetic flux  $\mathbf{B}$  are not independent from each other, nor are the dielectric displacement  $\mathbf{D}$  and the magnetic field  $\mathbf{H}$ . Mathematically, this is noticed from Maxwell's equations, especially, Eqs. (2) and (4). To resolve this problem, especially in the finite element formulation presented in the next section, let's introduce the scalar potential  $\phi$  and the vector potential  $\mathbf{A}$ , which are related to the electric field  $\mathbf{E}$  and magnetic flux  $\mathbf{B}$  as

$$\mathbf{B} \equiv \nabla \times \mathbf{A} \quad \text{or} \quad B_i = e_{ijk} A_{k,j} \quad (78)$$

$$\mathbf{E} \equiv -\nabla\phi - \frac{1}{c} \frac{\partial \mathbf{A}}{\partial t} \quad \text{or} \quad E_i \equiv -\phi_{,i} - \frac{1}{c} \frac{\partial A_i}{\partial t} \quad (79)$$

Now we follow the same pattern as Eqs. (61) and (62), and write the polarization  $P_k$ , magnetization  $M_k$ , and current  $J_k$  as

$$\begin{aligned} P_k &= D^1 E_k^* + D^3 B_k \\ M_k &= D^2 B_k + D^3 E_k^* \\ J_k &= g^2 \theta_{,k} + g^3 E_k^* \end{aligned} \quad (80)$$

Now the dielectric displacement vector  $\mathbf{D}$  and the magnetic field vector  $\mathbf{H}$  can be expressed as

$$\begin{aligned} D_k &= E_k + P_k \\ &= E_k + D^1 E_k^* + D^3 B_k \\ &= (1 + D^1) E_k + D^3 B_k + D^1 (E_k^* - E_k) \\ &\equiv \varepsilon E_k + D^3 B_k + D^1 (E_k^* - E_k) \\ &\approx \varepsilon E_k + D^3 B_k \end{aligned} \quad (81)$$

$$\begin{aligned} H_k &= B_k - M_k \\ &= B_k - (D^2 B_k + D^3 E_k^*) \\ &= (1 - D^2) B_k - D^3 E_k^* + D^3 (E_k^* - E_k) \\ &\equiv \mu^{-1} B_k - D^3 E_k^* + D^3 (E_k^* - E_k) \\ &\approx \mu^{-1} B_k - D^3 E_k \end{aligned} \quad (82)$$

Admittedly, the introduction of Eqs. (80)–(82) involve approximations. Without making these approximations, it is difficult, if not impossible, to derive the governing equations for the scalar potential  $\phi$  and vector potential  $\mathbf{A}$ .

Substituting Eqs. (78) and (79) into Maxwell's equations leads to

$$\begin{aligned} D_{k,k} &= \varepsilon E_{k,k} + D^3 B_{k,k} \\ &= -\varepsilon \left\{ \phi_{,kk} + \frac{1}{c} \dot{A}_{k,k} \right\} \\ &= q \end{aligned} \quad (83)$$

$$\nabla \times \mathbf{E} + \frac{1}{c} \frac{\partial \mathbf{B}}{\partial t} = \nabla \times \left\{ -\nabla \phi - \frac{1}{c} \dot{\mathbf{A}} \right\} + \frac{1}{c} \{ \nabla \times \dot{\mathbf{A}} \} = 0 \quad (84)$$

$$\nabla \cdot \mathbf{B} = \nabla \cdot (\nabla \times \mathbf{A}) = 0 \quad (85)$$

$$\begin{aligned} \nabla \times \mathbf{H} - \frac{1}{c} \frac{\partial \mathbf{D}}{\partial t} &= \nabla \times [\mu^{-1} \mathbf{B} - D^3 \mathbf{E}] - \frac{1}{c} \{ \varepsilon \dot{\mathbf{E}} + D^3 \dot{\mathbf{B}} \} \\ &= \mu^{-1} \nabla \times \mathbf{B} - \frac{\varepsilon}{c} \dot{\mathbf{E}} = \mu^{-1} \nabla \times \nabla \times \mathbf{A} + \frac{\varepsilon}{c} \left[ \nabla \dot{\phi} + \frac{1}{c} \ddot{\mathbf{A}} \right] \\ &= \frac{1}{c} \mathbf{J} \end{aligned} \quad (86)$$

It is seen that two of the four Maxwell's equations, Eqs. (84) and (85), are identically satisfied; the other two equations, Eqs. (83) and (86) can be rewritten as

$$\phi_{,kk} + \frac{1}{c} \dot{A}_{k,k} = -q/\varepsilon \quad (87)$$

$$\mu^{-1} [A_{j,ij} - A_{i,jj}] + \frac{\varepsilon}{c} \dot{\phi}_{,i} + \frac{\varepsilon}{c^2} \ddot{A}_i = \frac{1}{c} J_i \quad (88)$$

Following the same procedures in [8], the Lorentz condition is obtained as

$$\epsilon \frac{1}{c} \dot{\phi} + \mu^{-1} \nabla \cdot \mathbf{A} = 0 \tag{89}$$

Substituting the Lorentz condition into Eqs. (83) and (86) results

$$-\epsilon \left\{ \nabla^2 \phi + \frac{1}{c} \nabla \cdot \dot{\mathbf{A}} \right\} = -\epsilon \left\{ \nabla^2 \phi - \epsilon \mu \frac{1}{c^2} \ddot{\phi} \right\} = q \tag{90}$$

$$-\mu^{-1} \nabla^2 A_i + \frac{1}{c^2} \epsilon \ddot{A}_i = \frac{J_i}{c} \tag{91}$$

In other words, Maxwell's equations are reduced to

$$\epsilon \mu \frac{1}{c^2} \ddot{\phi} - \nabla^2 \phi = a \equiv \frac{q}{\epsilon} \tag{92}$$

$$\epsilon \mu \frac{1}{c^2} \ddot{A}_k - \nabla^2 A_k = C_k \equiv \frac{\mu}{c} J_k \tag{93}$$

This means the Maxwell's equations become two wave equations with forcing terms, and the speed of wave propagation is equal to

$$v = c / \sqrt{\epsilon \mu} \tag{94}$$

Since both the material constants  $\epsilon$  and  $\eta$  are positive and greater than one, therefore Eq. (94) says the speed of EM wave propagation in a material is lower than that in vacuum or in air.

### 7 Finite Element Formulation

Since the mechanical parts of the Lagrangian stress tensor and the Eulerian stress tensor are related as

$$T_{KL} = J t_{kl}^m X_{K,k} X_{L,l}, \quad t_{kl} = J^{-1} T_{KL}^m x_{k,K} x_{l,L} \tag{95}$$

One may verify that the balance law of linear momentum, Eq. (19), can be rewritten as

$$(T_{KL}^m x_{l,L})_{,K} + \rho^o (f_l - \dot{v}_l) + J F_l = 0 \tag{96}$$

The law of conservation of energy can be written as [7]

$$\rho^o \dot{e} = T_{KL}^m \dot{E}_{KL} - Q_{K,K} - P_K \dot{E}_K^* - M_K^* \dot{B}_K + J_K^* E_K^* - \rho^o h \tag{97}$$

Based on the constitutive equations, Eqs. (59)–(62), (65)–(67) and (97) can be further derived to be [7]

$$\begin{aligned} & \rho^o \gamma \frac{T + T^o}{T^o} \dot{T} + (T + T^o) \bar{A}_{KL} \dot{E}_{KL}^e \\ & = T_{KL}^{me} \dot{E}_{KL}^p + T_{KL}^d \dot{E}_{KL} - Q_{K,K} - P_K \dot{E}_K^* - M_K^* \dot{B}_K + J_K^* E_K^* + \rho^o h \end{aligned} \tag{98}$$

Recall the governing equations of the scalar potential  $\phi$  and the vector potential  $\mathbf{A}$  as

$$\frac{\epsilon \mu}{c^2} \ddot{\phi} - \nabla^2 \phi = \frac{q}{\epsilon} \equiv a \tag{99}$$

$$\varepsilon\mu\frac{1}{c^2}\ddot{A}_k - \nabla^2 A_k = C_k \equiv \frac{\mu}{c} \{g^2\theta_{,k} + g^3 E_k^*\} \quad (100)$$

We now link the displacement, temperature, scalar potential, and vector potential at a generic point in an element to the corresponding nodal values associated with this element as follows:

$$\begin{aligned} U_K &= N_\alpha U_{K\alpha} \\ T &= N_\alpha T_\alpha \\ \phi &= N_\alpha \phi_\alpha \\ A_k &= N_\alpha A_{k\alpha} \end{aligned} \quad (101)$$

where  $N_\alpha [\alpha = 1, 2, 3, \dots, 8]$  are the 8 shape functions for a standard 8-node 3D element. The finite element equations are obtained as (for detailed derivation, see [Appendix A](#))

$$M_{\alpha\beta} \ddot{U}_{M\beta} = f_{M\alpha}^1 + f_{M\alpha}^2 + f_{M\alpha}^3 \quad (102)$$

$$\gamma M_{\alpha\beta} \dot{T}_\beta = q_\alpha^1 + q_\alpha^2 + q_\alpha^3 + q_\alpha^4 + q_\alpha^5 + q_\alpha^6 + q_\alpha^7 \quad (103)$$

$$m_{\alpha\beta} \ddot{\phi}_\beta + k_{\alpha\beta} \phi_\beta = \hat{\xi}_\alpha + \tilde{a}_\alpha \quad (104)$$

$$m_{\alpha\beta} \ddot{A}_{k\beta} + k_{\alpha\beta} A_{k\beta} = \hat{A}_{k\alpha} + \hat{C}_{k\alpha} \quad (105)$$

where

$$M_{\alpha\beta} \equiv \int_V \rho^0 N_\alpha N_\beta dV = M_{\beta\alpha} \quad (106)$$

$$\gamma M_{\alpha\beta} \equiv \int_V \rho^0 \gamma N_\alpha N_\beta dV = \gamma M_{\beta\alpha} \quad (107)$$

$$m_{\alpha\beta} \equiv \int_V \frac{1}{c^2} N_\alpha N_\beta dV \quad (108)$$

$$k_{\alpha\beta} \equiv \int_V N_{\alpha,i} N_{\beta,i} dV \quad (109)$$

and  $f_{m\alpha}^1, f_{m\alpha}^2, f_{m\alpha}^3, q_\alpha^1, q_\alpha^2, q_\alpha^3, q_\alpha^4, q_\alpha^5, q_\alpha^6, q_\alpha^7, \hat{\xi}_\alpha, \tilde{a}_\alpha, \hat{A}_{k\alpha}$ , and  $\hat{C}_{k\alpha}$  are defined in [Appendix A](#).

## 8 Torsion Problem

It is noticed that (a) [Eq. \(96\)](#) is mainly a governing equation for displacement  $\mathbf{u}$  and it is a wave equation, (b) [Eq. \(98\)](#) is mainly a governing equation for temperature  $T$  and it is a diffusion equation, (c) [Eq. \(99\)](#) is a wave equation for scalar potential  $\phi$ , (d) [Eq. \(100\)](#) is a wave equation for the vector potential  $\mathbf{A}$ . Of course, all those differential equations have forcing terms that make  $\mathbf{u}$ ,  $T$ ,  $\phi$ , and  $\mathbf{A}$  coupled together—that is why it is coined with the name thermomechanical–electromagnetic coupling.

However, we also noticed that the wave speed for the scalar potential  $\phi$  and the vector potential  $\mathbf{A}$  is equal to  $c/\sqrt{\varepsilon\mu}$  which, for most materials, is at the same order as the speed of light; and yet the wave speed for the displacement is just the speed for an acoustic wave in the material; the speed involved in the diffusion equation is related to the thermal conductivity. Therefore, we consider solving the four differential equations, [Eqs. \(96\) and \(98\)–\(100\)](#), simultaneously, is numerically difficult (if not impossible) and physically meaningless. We propose to solve this problem in two stages.

In this work, we are using the MKS system, i.e., meter, kilogram, and second are the units for length, mass, and time, respectively. Also, let the units of temperature and electric charge be  $^{\circ}K$  and  $q$ , respectively. In the Heaviside-Lorentz system, the dimensions of the electric field and the magnetic field are  $[E] = [B] = KM/s^2/q$ . The numerical values of the material constants are specified as

$$\begin{aligned} \bar{A} &= 0.002 K/M/s^2/^{\circ}K \\ \lambda^1 &= 6 K/M/s^2, \quad \mu^{11} = 4.5 K/M/s^2, \quad \mu^{12} = 1.5 K/M/s^2 \\ \bar{\lambda}^1 &= 0.03 K/M/s, \quad \bar{\mu}^{11} = 0.0225 K/M/s, \quad \bar{\mu}^{12} = 0.0075 K/M/s \\ E_Y &= 10000, \quad \kappa = 1, \quad H = 5, \quad C_1 = 0.6, \quad C_2 = 0.4 \\ \gamma &= 400000 M^2/s^2/^{\circ}K, \quad T^{\circ} = 300^{\circ}K \\ g^1 &= 2000 KM/s^3/^{\circ}K, \quad g^2 = 10 M/s/^{\circ}K, \quad g^3 = 10/s \\ \rho^{\circ} &= 1000 K/M^3, \quad \varepsilon = 2, \quad \mu = 2 \end{aligned} \quad (110)$$

### **Numerical Results of the Torsion Problem**

Let the specimen be a hollow cylinder occupying

$$V = \{R, \theta, Z | 1.0 \leq R \leq 2.0, \quad 0 \leq \theta \leq 2\pi, \quad 0 \leq Z \leq 30\} \quad (111)$$

The finite element mesh has 2520 nodes and 1920 8-node solid elements. In Stage I, each node has 4 unknowns (three for  $\mathbf{U}$  and one for  $T$ ), this sample problem has 10,080 degrees of freedom. Here, Heun's method is employed to solve Eqs. (96) and (98), which are one wave equation and one diffusion equation. This work consists of two approaches, each of which has two stages.

#### **First Approach**

To ensure numerical stability, the time step  $\Delta t$  cannot be too large. For this sample problem, in Stage I, we use  $\Delta t = 0.004$  s and have verified that such  $\Delta t$  not only provides stability but also accuracy.

The boundary conditions are specified as:

(I) At the top surface,  $Z = 30$

$$\begin{aligned} U_x &= r \cos(\theta + \Delta\theta) - X, \quad U_y = r \sin(\theta + \Delta\theta) - Y, \quad U_z = 3.0 \\ T &= 5.0 \end{aligned} \quad (112)$$

where  $\Delta\theta = 0.25\pi$  and

$$r \equiv \sqrt{X^2 + Y^2}, \quad \theta = \tan^{-1}(Y/X) \quad (113)$$

This means all the nodes on the top surface are rotated by  $45^{\circ}$  counterclockwise, and the temperature variation is specified at  $5^{\circ}K$ .

(II) At the bottom surface,  $Z = 0$

$$U_x = U_y = U_z = T = 0 \quad (114)$$

The corresponding system of equations, Eqs. (96) and (98), statically can be expressed as

$$f_{M\alpha}^1 + f_{M\alpha}^2 + f_{M\alpha}^3 = 0 \quad \text{or} \quad \mathbf{f}(\mathbf{U}, \mathbf{T}) = 0 \quad (115)$$

$$q_{\alpha}^1 + q_{\alpha}^2 + q_{\alpha}^3 + q_{\alpha}^4 + q_{\alpha}^5 + q_{\alpha}^6 + q_{\alpha}^7 = 0 \quad \text{or} \quad \mathbf{q}(\mathbf{U}, \mathbf{T}) = 0 \quad (116)$$

Usually, we would solve Eqs. (117) and (118) by using the Newton-Raphson method. Since, in the finite element analysis of this simple model, there are 10,080 degrees of freedom. In this case, the Newton-Raphson method involves a stiffness matrix of size  $10,020 \times 10,020$ . This means it is practically impossible to solve it by the Newton-Raphson method. Another way is to solve Eqs. (96) and (98) dynamically with proper damping coefficients so that, with a reasonable number of time steps, one may obtain nearly static solutions.

Since the Cauchy stress tensor and the corresponding 2nd order Piola-Kirchhoff stress are symmetric, the  $L_2$ -norm of the 2nd order Piola-Kirchhoff stress is defined as

$$VON \equiv \{T_{KL}T_{KL}\}^{\frac{1}{2}} \equiv \sqrt{T_{11}^2 + T_{22}^2 + T_{33}^2 + 2T_{23}^2 + 2T_{31}^2 + 2T_{12}^2} \quad (117)$$

Similarly, the  $L_2$ -norm of the plastic strain  $\mathbf{E}^p$  is defined as

$$P_{avg} \equiv \{E_{KL}^p E_{KL}^p\}^{1/2} = \sqrt{E_{11}^p E_{11}^p + E_{22}^p E_{22}^p + E_{33}^p E_{33}^p + 2E_{23}^p E_{23}^p + 2E_{31}^p E_{31}^p + 2E_{12}^p E_{12}^p} \quad (118)$$

The finite element results, i.e.,  $TEM \equiv$  Temperature Variation,  $P_{avg}$ , and  $VON$ , of Stage I are plotted on the deformed shape in Fig. 1. It is observed that  $TEM$ ,  $P_{avg}$ , and  $VON$  are indeed axis-symmetric. Actually, one may utilize *Tecplot* to show each component of plastic strain and each component of Piola-Kirchhoff stress.

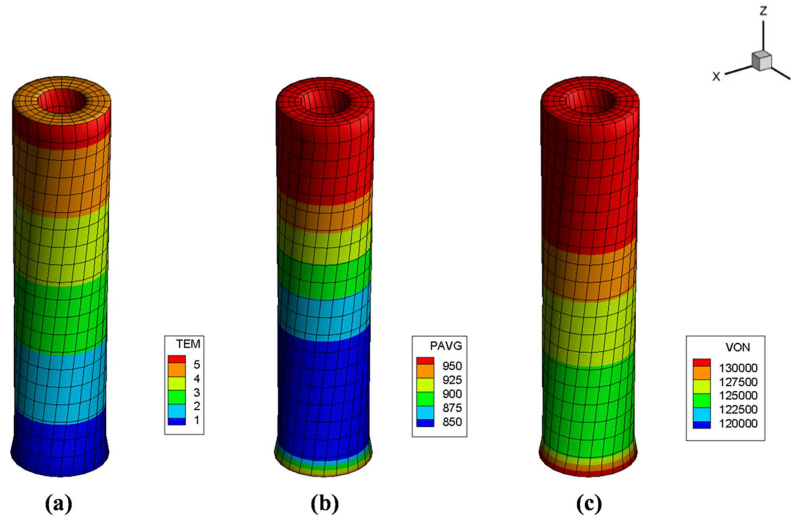


**Figure 1:** (a) Temperature Variation, (b)  $L_2$ -norm of the plastic strain, (c)  $L_2$ -norm of the 2nd order Piola-Kirchhoff stress. The color bars show the magnitudes of those variables. From the mesh, one can observe the deformed shape and also the axis symmetry. In Stage II, we investigate four cases. The boundary conditions at the bottom surface and the top surface are specified as follows.

**Case 1**  $A_y = A_z = \phi = 0$

Bottom Surface

$$A_x = \begin{cases} V \sin \left\{ \frac{\pi t}{100\Delta t} \right\} & \text{if } t \leq 400\Delta t \\ 0 & \text{if } t \geq 400\Delta t \end{cases} \quad (119)$$

Top Surface

$$A_x = 0 \quad (120)$$

It means all nodes on the bottom surface are excited with a sine wave having a finite period of time ( $400 \Delta t$ ) is propagating toward the top surface and then bounces back.

**Case 2**  $A_x = A_z = \phi = 0$

Bottom Surface

$$A_y = \begin{cases} V \sin \left\{ \frac{\pi t}{100 \Delta t} \right\} & \text{if } t \leq 400 \Delta t \\ 0 & \text{if } t \geq 400 \Delta t \end{cases} \quad (121)$$

Top Surface

$$A_y = 0 \quad (122)$$

**Case 3**  $A_x = A_y = \phi = 0$

Bottom Surface

$$A_z = \begin{cases} V \sin \left\{ \frac{\pi t}{100 \Delta t} \right\} & \text{if } t \leq 400 \Delta t \\ 0 & \text{if } t \geq 400 \Delta t \end{cases} \quad (123)$$

Top Surface

$$A_z = 0 \quad (124)$$

**Case 4**  $A_x = A_y = A_z = 0$

Bottom Surface

$$\phi = \begin{cases} V \sin \left\{ \frac{\pi t}{100 \Delta t} \right\} & \text{if } t \leq 400 \Delta t \\ 0 & \text{if } t \geq 400 \Delta t \end{cases} \quad (125)$$

Top Surface

$$\phi = 0 \quad (126)$$

In Eqs. (119), (121), (123) and (125), the numerical value of  $V$  equals one, and the dimension is  $\text{KM}^2/\text{s}^2/\text{q}$ . It is worthwhile to mention that the time step in Stage II is  $\Delta t = 0.25 \times 10^{-9}$  s, comparing with  $\Delta t = 0.004$  s in Stage I. This huge difference justifies the treatment of the thermomechanical electromagnetic coupling problem by a two-stage solution procedure. It should be emphasized that since  $A_x, A_y, A_z, \phi$  are mutually independent of each other, the four cases are mutually independent of each other. Recall Eqs. (127) and (128)

$$\mathbf{B} = \nabla \times \mathbf{A} \quad (127)$$

$$\mathbf{E} = -\nabla \phi - \frac{1}{c} \frac{\partial \mathbf{A}}{\partial t} \quad (128)$$

and one may find that  $\{A_x, B_y, B_z, E_x\}$ ,  $\{A_y, B_z, B_x, E_y\}$ ,  $\{A_z, B_x, B_y, E_z\}$ ,  $\{\phi, B_x, B_y, B_z\}$  are the unknown variables in the four cases, respectively. The numerical results of  $\phi, \mathbf{A}, \mathbf{E}, \mathbf{B}$  as functions of time of the four cases are shown in Figs. 2–5, respectively.

From the color bars of the four figures, one may observe the wave propagation of the scalar potential  $\phi$  and vector potential  $A_k$ , as well as the induced electric field vector  $E_k$  and magnetic induction vector  $B_k$ . It is noticed that the waves started at the bottom surface and reflected back from the top surface.

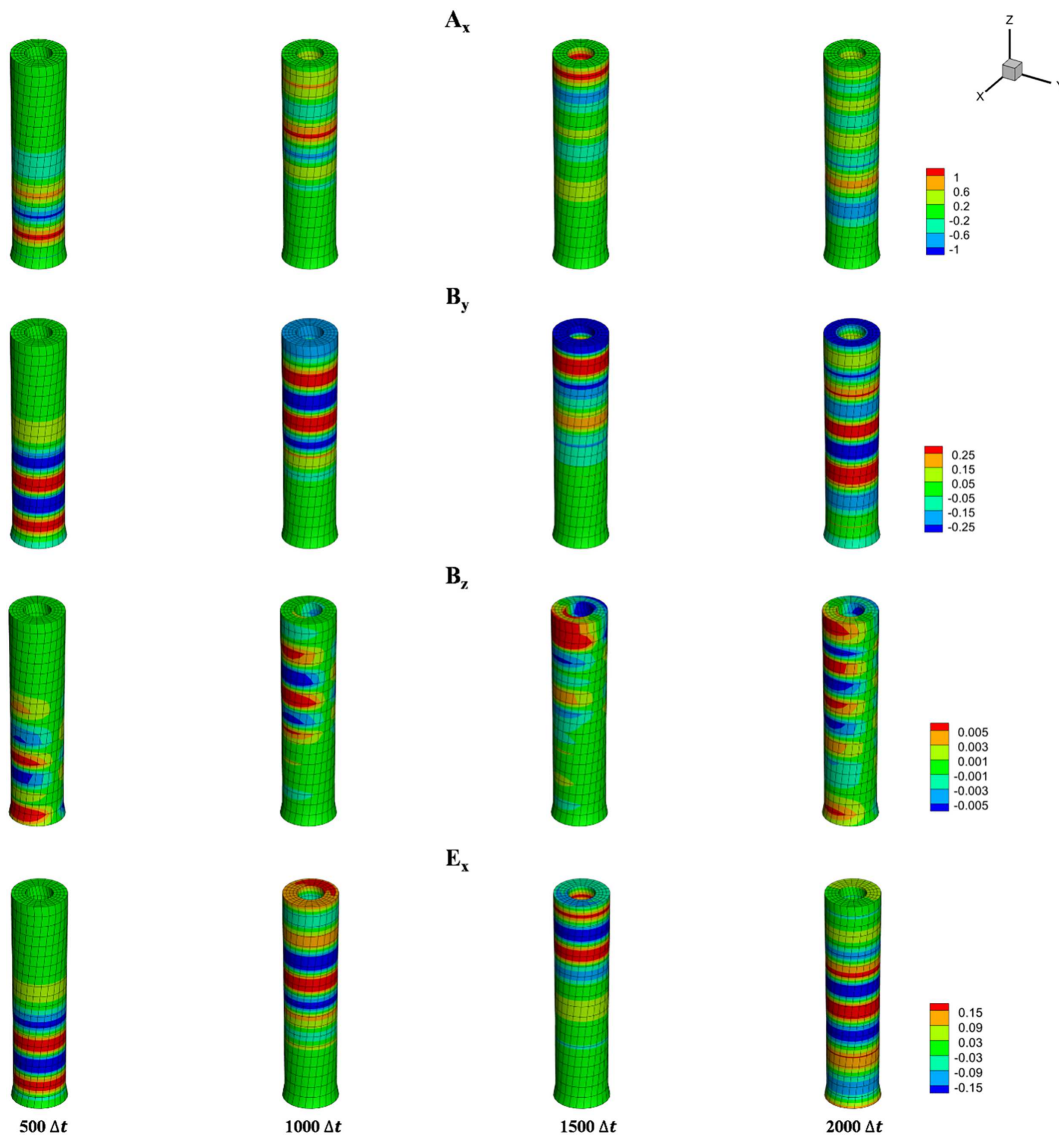


**Figure 2:** The first row is  $A_x$ , the second row is  $B_y$ , the third row is  $B_z$ , the fourth row is  $E_x$ . The first, second, third, fourth column is the data at  $500 \Delta t$ ,  $1000 \Delta t$ ,  $1500 \Delta t$ ,  $2000 \Delta t$ , respectively. The color bars show the magnitudes of the variables. As time processes one may observe the wave propagation, including the bouncing back of the wave.

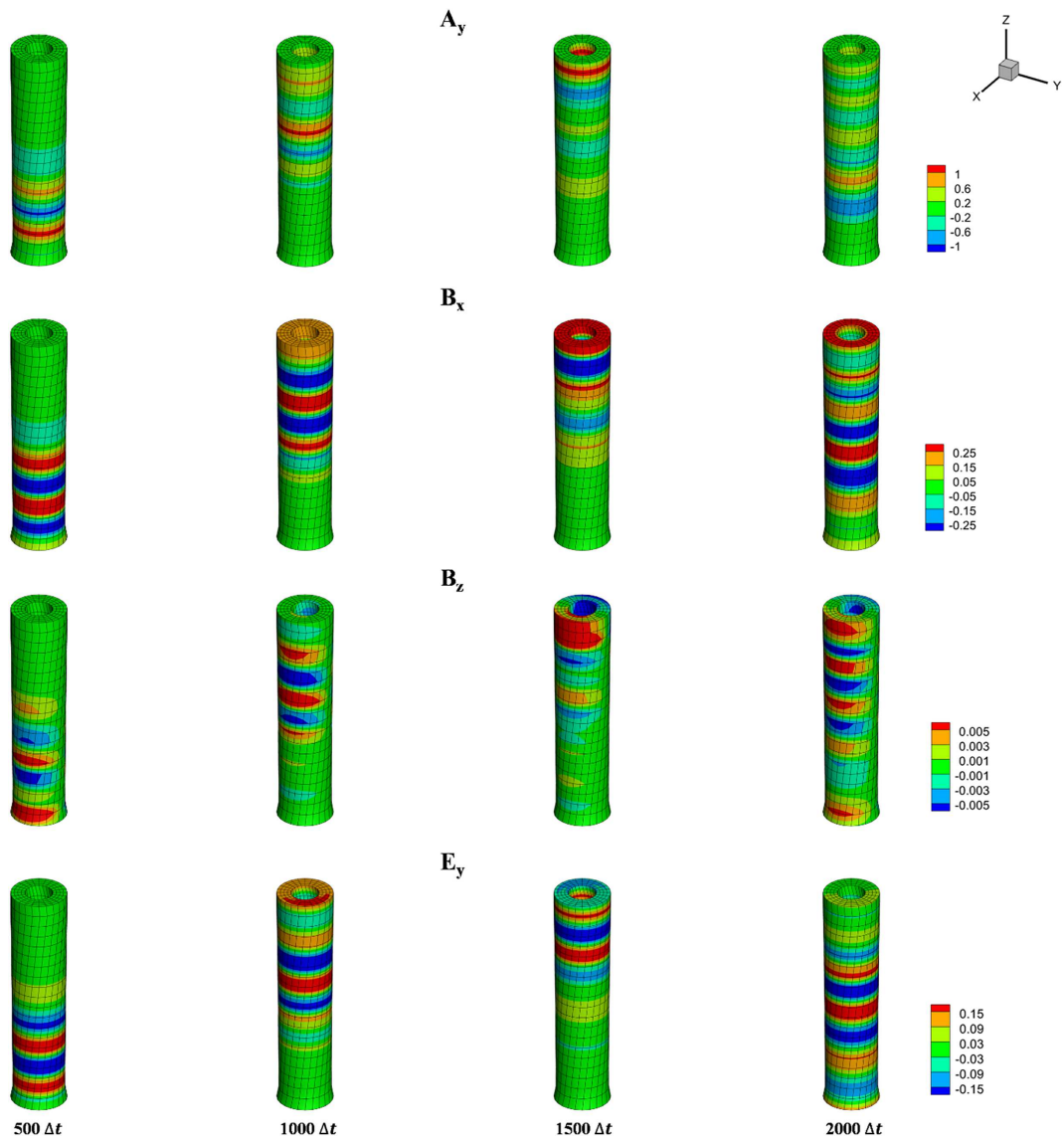


**Figure 3:** The first row is  $A_y$ , the second row is  $B_x$ , the third row is  $B_z$ , the fourth row is  $E_y$ . The first, second, third, and fourth columns are the data at  $500 \Delta t$ ,  $1000 \Delta t$ ,  $1500 \Delta t$ ,  $2000 \Delta t$ , respectively. The color bars show the magnitudes of the variables. As time progresses, one may observe the wave propagation, including the bouncing back of the wave.

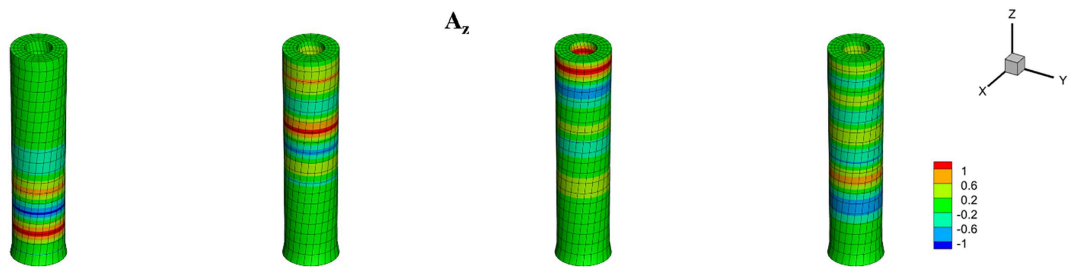


**Figure 4:** (Continued)

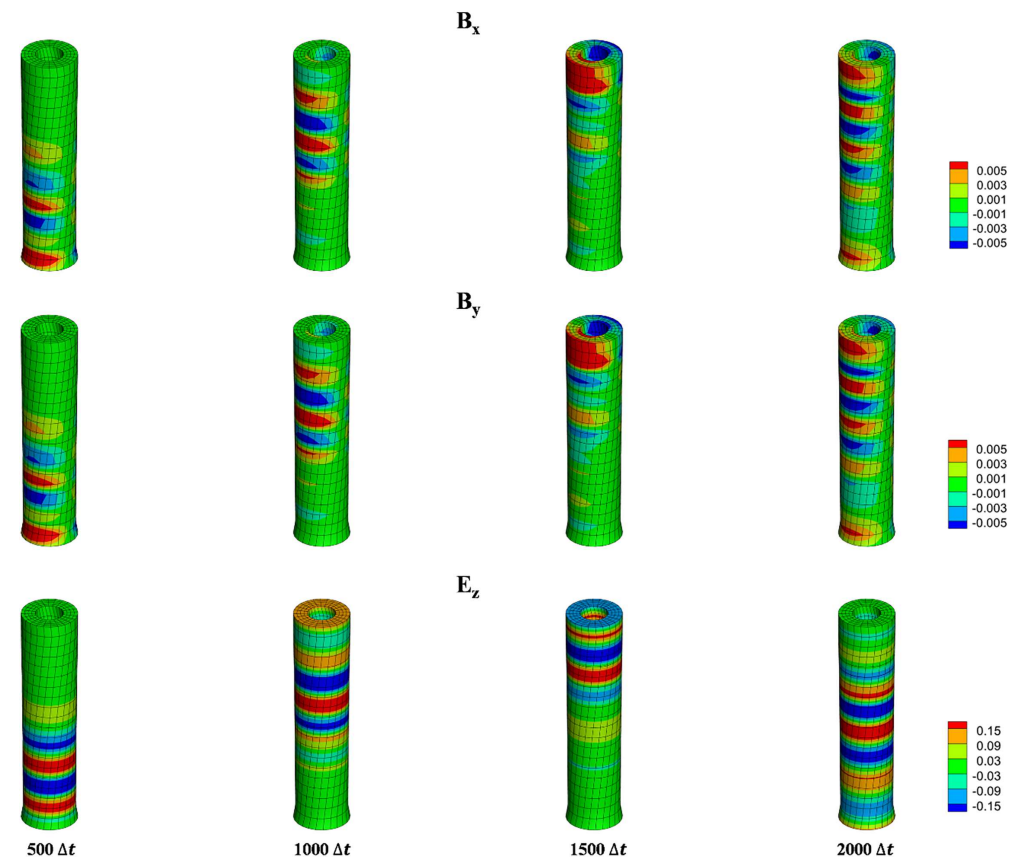


**Figure 4:** The first row is  $A_z$ , the second row is  $B_x$ , the third row is  $B_y$ , the fourth row is  $E_z$ . The first, second, third, and fourth columns are the data at  $500 \Delta t$ ,  $1000 \Delta t$ ,  $1500 \Delta t$ ,  $2000 \Delta t$ , respectively. The color bars show the magnitudes of the variables. As time progresses, one may observe the wave propagation, including the bouncing back of the wave.

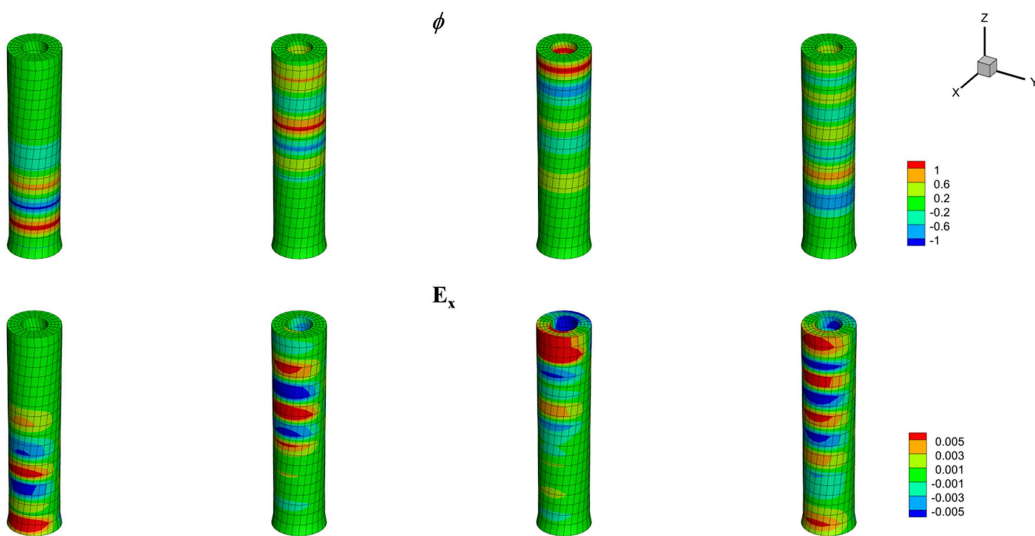


**Figure 5:** (Continued)

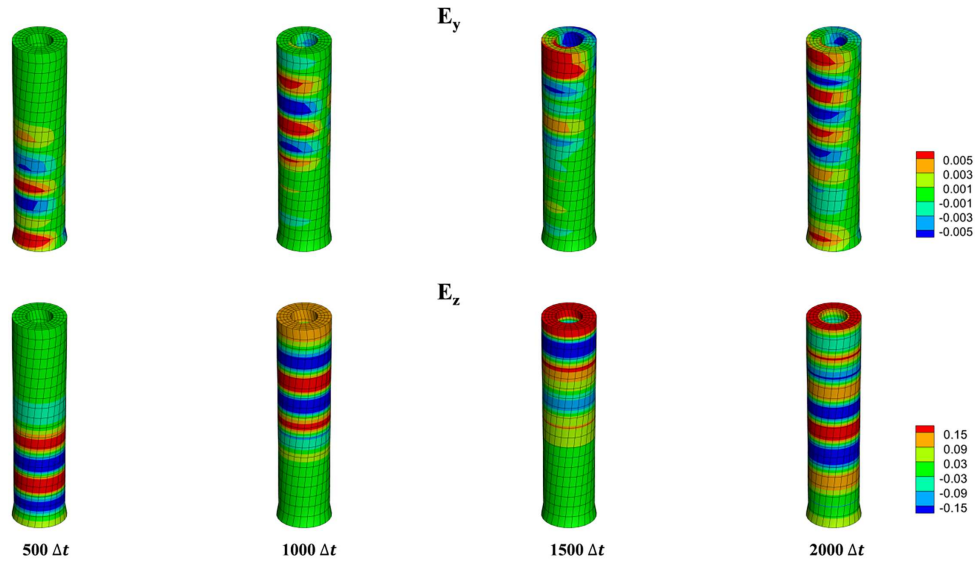


**Figure 5:** The first row is  $\phi$ , the second row is  $E_x$ , the third row is  $E_y$ , the fourth row is  $E_z$ . The first, second, third, and fourth columns are the data at  $500 \Delta t$ ,  $1000 \Delta t$ ,  $1500 \Delta t$ ,  $2000 \Delta t$ , respectively. The color bars show the magnitudes of the variables. As time progresses, one may observe the wave propagation, including the bouncing back of the wave.

**Second Approach**

In the second approach, the first stage solutions are obtained for static scalar and vector potentials. Then Eqs. (102) and (103) are solved for dynamic solutions of displacements and temperatures with forcing terms obtained from the first stage solutions. There are four independent cases:

Case 1  $A_y = A_z = \phi = 0$

$$A_x = A_x(x, y, z) \tag{129}$$

Case 2  $A_x = A_z = \phi = 0$

$$A_y = A_y(x, y, z) \tag{130}$$

Case 3  $A_x = A_y = \phi = 0$

$$A_z = A_z(x, y, z) \tag{131}$$

Case 4  $A_x = A_y = A_z = 0$

$$\phi = \phi(x, y, z) \tag{132}$$

First, it is noticed that these four cases are static cases. Following the static cases of Eqs. (78) and (79), we have

$$\mathbf{B} = \nabla \times \mathbf{A}, \quad \mathbf{E} = -\nabla\phi \tag{133}$$

Then, for the four cases we have

Case 1

$$B_y = \frac{\partial A_x}{\partial z}, \quad B_z = -\frac{\partial A_x}{\partial y} \quad (134)$$

Case 2

$$B_x = -\frac{\partial A_y}{\partial z}, \quad B_z = \frac{\partial A_y}{\partial x} \quad (135)$$

Case 3

$$B_x = \frac{\partial A_z}{\partial y}, \quad B_y = -\frac{\partial A_z}{\partial x} \quad (136)$$

Case 4

$$E_x = -\frac{\partial \phi}{\partial x}, \quad E_y = -\frac{\partial \phi}{\partial y}, \quad E_z = -\frac{\partial \phi}{\partial z} \quad (137)$$

One may also verify that Eqs. (134)–(137) satisfy  $\nabla \cdot \mathbf{B} = 0$  and  $\nabla \times \mathbf{E} = 0$ , which are the two static homogeneous equations of Maxwell's equations. In Eqs. (129)–(132), the dimension of  $(A_x, A_y, A_z, \phi)$  is  $\text{KM}^2/\text{s}^2/\text{q}$ . It should be emphasized that  $A_x, A_y, A_z, \phi$  are mutually independent of each other. Also, it is seen that the static electric field  $\mathbf{E}$  and the static magnetic field  $\mathbf{B}$  are mutually independent of each other. The generality of the *Stage I* solution is seen in Eqs. (129)–(132). On the other hand, one could simplify those equations so that analytical solutions are obtained.

In *Stage II*, each node has 4 unknowns (three for  $\mathbf{U}$  and one for  $T$ ), this sample problem has 10,080 degrees of freedom. Here, Heun's method is employed to solve Eqs. (96) and (98), which are one wave equation and one diffusion equation. To ensure numerical stability, the time step  $\Delta t$  cannot be too large. For this sample problem, in *Stage II*, we use  $\Delta t = 0.000005$  s and have verified that such  $\Delta t$  not only provides stability but also accuracy.

The boundary conditions are specified as:

(I) At the top surface,  $Z = 30$

$$U_x = r \cos(\theta + \Delta\theta) - X, \quad U_y = r \sin(\theta + \Delta\theta) - Y, \quad U_z = \Delta L \\ T = 5.0 \quad (138)$$

where  $r \equiv \sqrt{X^2 + Y^2}$ ,  $\theta = \tan^{-1}(Y/X)$ ,

$$\Delta\theta = \begin{cases} \frac{\pi}{4} \frac{t}{t_{\max}}, & t \leq t_{\max} \\ \frac{\pi}{4}, & t > t_{\max} \end{cases}, \quad \Delta L = \begin{cases} 3.0 \frac{t}{t_{\max}}, & t \leq t_{\max} \\ 3.0, & t > t_{\max} \end{cases} \quad (139)$$

This means all the nodes on the top surface are rotated by  $45^\circ$  counterclockwise and elongated by 3.0 linearly up to  $t_{\max}$  and stay there. The temperature variation is specified at  $5^\circ\text{K}$ . In this work  $t_{\max} = 7000 * \Delta t$ .

(II) At the bottom surface,  $Z = 0$

$$U_x = U_y = U_z = T = 0 \quad (140)$$

The governing equations for the displacement fields  $\mathbf{U}$  and the temperature fields  $\mathbf{T}$ , Eqs. (96) and (98), can be rewritten as (A9) and (A19), where  $f_{M\alpha}^i \{i = 1, 2, 3\}$  and  $q_\alpha^j \{j = 1, 2, 3, 4, 5, 6, 7\}$  are defined in Appendix A. It is understood that the details of  $f_{M\alpha}^i$  and  $q_\alpha^j$  should be consistent with the *Stage I* solutions, i.e., the static electric solution  $\mathbf{E}$ , Eq. (137), or the static magnetic solution  $\mathbf{B}$ , Eqs. (134) or (135) or (136).

In this work, we only look for solutions of Case 3 and Case 4—the typical representative cases with axis symmetry. The finite element results, wave propagation of the displacement field, and diffusion process of the temperature field, are plotted on the deformed shape in Figs. 6 and 7. It is noticed that the temperature, plastic strains, von Mises stresses, and current vectors are independent of the static magnetic field because  $f_{M\alpha}^i \{i = 1, 2, 3\}$  and  $q_\alpha^j \{j = 1, 2, 3, 4, 5, 6, 7\}$  in Eqs. (A9) and (A19) are independent of the static magnetic field. Notice that  $TEM \equiv$  Temperature Variation,  $VON$  and  $P_{avg}$  are defined in Eqs. (117) and (118). In Fig. 6, the  $TEM$ ,  $L2$ -norms of  $P_{avg}$  and  $VON$  are plotted as functions of time. The current in the  $z$ -direction due to the input of the static electric field are plotted as functions of time in Fig. 7.

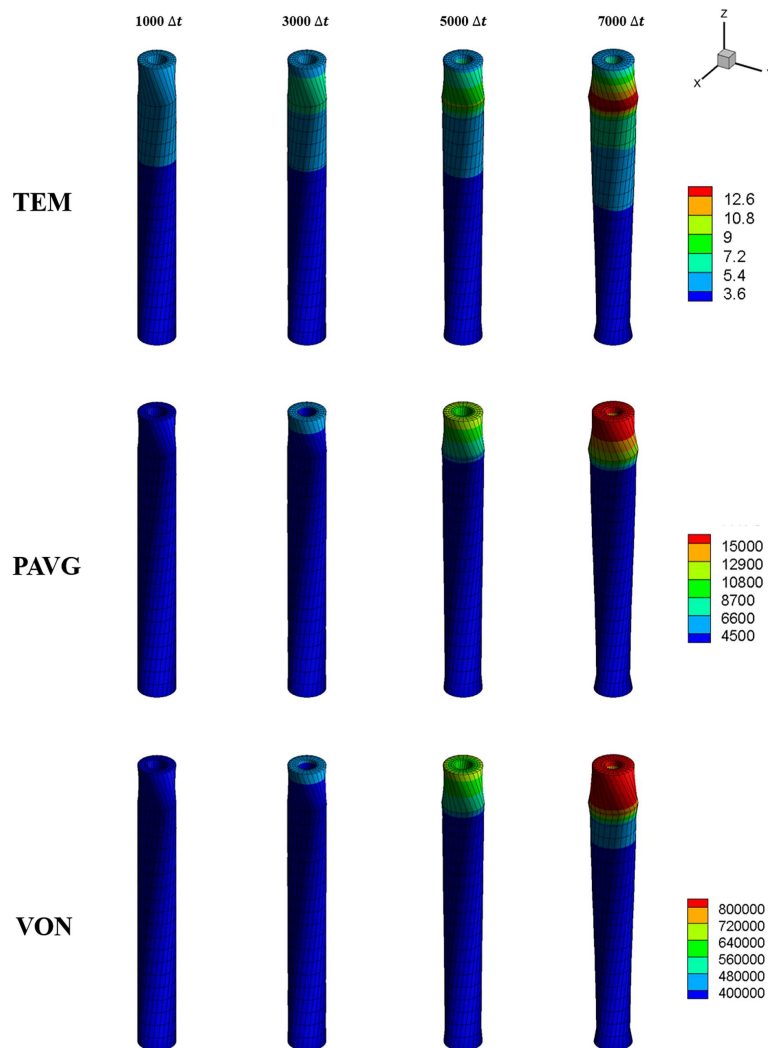


**Figure 6:** The first row is the temperature, the second row is the  $L2$ -norm of the plastic strain, and the third row is the  $L2$ -norm of the von Mises stress. The first, second, third, and fourth columns are the data at  $1000 \Delta t$ ,  $3000 \Delta t$ ,  $5000 \Delta t$ ,  $7000 \Delta t$ , respectively. The color bars show the magnitudes of the variables. The time processes show the diffusion process of the temperature, the propagation of the plastic strain, and the von Mises stress.

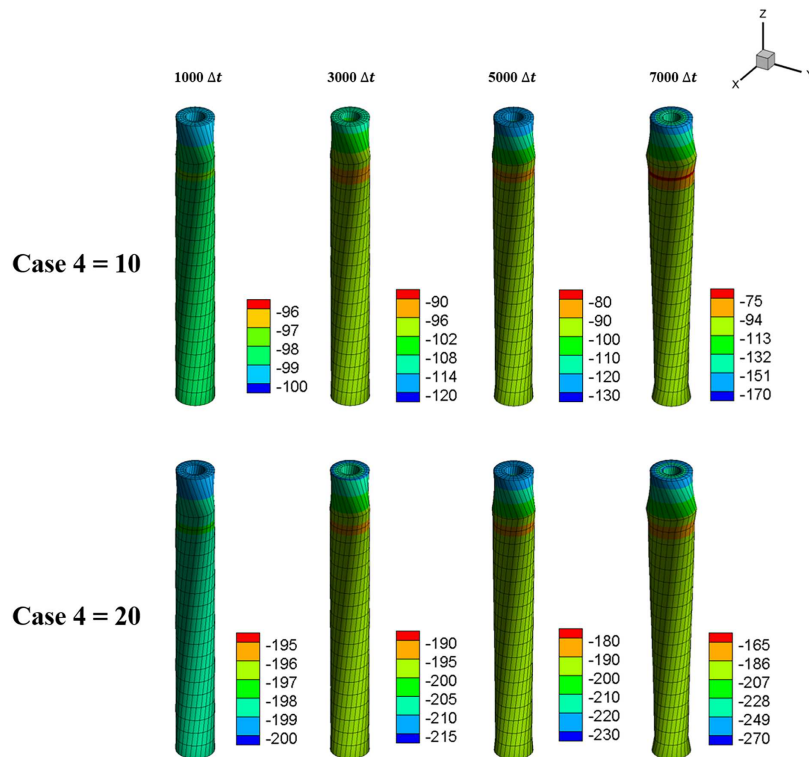


**Figure 7:** The first row is the current in the z-direction due to the electric field with Case 4 = 10. The second row is the current in the z-direction due to the electric field with Case 4 = 20. The first, second, third, fourth column is the 1000  $\Delta t$ , 3000  $\Delta t$ , 5000  $\Delta t$ , 7000  $\Delta t$ , respectively. The color bars show the magnitudes of the variables. The mesh enables one to observe the axis-symmetry.

## 9 Discussion

After the finite element formulation, we end up with the governing equations (Eqs. (102)–(105)) for temperature, displacements, scalar and vector potentials. The governing equations for displacements are wave equations for acoustic waves, and the equations for scalar and vector potentials are wave equations for optic wave. The wave speeds for acoustic waves and optical waves are so huge that to solve those equations simultaneously is numerically difficult (if not impossible) and physically meaningless. Therefore, we propose a two-stage solution method that can be performed in two approaches.

In Approach 1, we solve the static (or nearly static) thermomechanical problem in *Stage I*. The solution of the problem in Stage I will serve as forcing terms for scalar and vector potentials in *Stage II*. Both sets of solutions are presented.

In Approach 2, we solve the static scalar or vector potential problem in *Stage I*. In a static problem, the speed is zero. Then the scalar or vector potential serves as the forcing terms for temperature and displacements in *Stage II*. Both sets of solutions are presented.

The finite element program has been developed in-house. Many subroutines have been developed more than a decade ago. We have also built in many checkpoints. A mistake will stop the running of the computer code. For example, if a mistake is encountered in the return mapping algorithm, the entire code will be stopped. Therefore, no mistake is associated with the plasticity in this work. Finally, it is worthwhile to name a few references for future work [14–18].

## 10 Conclusion

First, we introduce Maxwell’s equations and the balance laws of classical continuum mechanics. These two sets of equations are linked together through the electromagnetic part of the body force, body moment, and energy source (cf. Eqs. (23)–(25)). Then we derive the constitutive equations for a geometrically nonlinear thermo-visco-elastic-plastic-electromagnetic continuum. We realize that the electric field  $\mathbf{E}$  and magnetic flux  $\mathbf{B}$  are not independent of each other; one must rely on the introduction of the scalar potential  $\phi$  and vector potential  $\mathbf{A}$  with the relation between  $\{\phi, \mathbf{A}\}$  and  $\{\mathbf{E}, \mathbf{B}\}$  (cf. Eqs. (78) and (79)). Then we formulate the coupled finite element equations for the temperature, displacement, scalar potential, and vector potential fields. The finite element equations for the displacement field are acoustic wave equations, and the finite element equations for the scalar and vector potentials are optic wave equations. The wave speeds of the two sets of finite element equations have a huge difference. To solve these equations simultaneously is numerically difficult (if not impossible) and physically meaningless. This is considered the greatest limitation of this work. Therefore, we propose to solve this problem in two approaches, each of which has two stages. The details are described in Section 8.

**Acknowledgement:** None.

**Funding Statement:** The authors received no specific funding for this study.

**Author Contributions:** Shuaiqi Song contributed to Methodology, Investigation, Visualization, Validation, and Writing—original draft. Lijie Grace Zhang contributed to Supervision, Funding acquisition, Writing—review and editing. James D. Lee contributed to Conceptualization, Formal analysis, Supervision, Writing—review and editing. All authors reviewed and approved the final version of the manuscript.

**Availability of Data and Materials:** Data available on request from the authors. The data that support the findings of this study are available from the corresponding author, upon reasonable request.

**Ethics Approval:** Not applicable.

**Conflicts of Interest:** The authors declare no conflicts of interest.

## Appendix A

First, we link the displacement, temperature, scalar potential, and vector potential at a generic point in an element to the corresponding nodal values associated with this element as follows:

$$\begin{aligned} U_K &= N_\alpha U_{K\alpha}, & T &= N_\alpha T_\alpha \\ \phi &= N_\alpha \phi_\alpha, & A_k &= N_\alpha A_{k\alpha} \end{aligned} \tag{A1}$$

The weak form of Eq. (96) can be written as

$$\int_V \{T_{KL}^m x_{l,L}\}_{,K} + \rho^o (f_l - \dot{v}_l) + JF_l\} \delta u_l dV = 0 \tag{A2}$$

Term by term, we may obtain the followings:

$$\begin{aligned}
 \int_V (T_{KL}^m x_{l,K})_{,K} \delta u_l dV &= \oint_S T_{KL}^m x_{l,L} n_K \delta u_l dS - \int_V T_{KL}^m x_{l,L} \delta u_{l,K} dV \\
 &= \delta U_{M\alpha} \left\{ \oint_S T_{KL}^m x_{l,L} n_K \delta_{lM} N_\alpha dS - \int_V T_{KL}^m x_{l,L} \delta_{lM} N_{\alpha,K} dV \right\} \\
 &= \delta U_{M\alpha} \left\{ \int_{S_\sigma} \hat{F}_M N_\alpha dS - \int_V T_{KL}^m x_{l,L} \delta_{lM} N_{\alpha,K} dV \right\} \tag{A3}
 \end{aligned}$$

where on the boundary,  $S_\sigma$ , the surface force is specified as

$$\hat{F}_M = T_{KL}^m x_{l,L} n_K \delta_{lM} \tag{A4}$$

Also, we define

$$f_{M\alpha}^1 \equiv \int_{S_F} \hat{F}_M N_\alpha dS, \quad f_{M\alpha}^2 \equiv - \int_V T_{KL}^m x_{l,L} \delta_{lM} N_{\alpha,K} dV \tag{A5}$$

The other two terms are derived to be

$$\int_V (\rho^\circ f_l + JF_l) \delta u_l dV = \delta U_{M\alpha} \int_V (\rho^\circ f_M + JF_M) N_\alpha dV \equiv \delta U_{M\alpha} f_{M\alpha}^3 \tag{A6}$$

$$\int_V \rho^\circ \dot{v}_l \delta u_l dV = \ddot{U}_{M\beta} \delta U_{M\alpha} \int_V \rho^\circ N_\alpha N_\beta dV \equiv \ddot{U}_{M\beta} \delta U_{M\alpha} M_{\alpha\beta} \tag{A7}$$

Now Eq. (A2) can be re-written as

$$\delta U_{M\alpha} \{ f_{M\alpha}^1 + f_{M\alpha}^2 + f_{M\alpha}^3 - M_{\alpha\beta} \ddot{U}_{M\beta} \} = 0 \tag{A8}$$

Because Eq. (A8) has to be valid for arbitrary virtual displacement  $\delta U_{M\alpha}$ , the finite element equation for the balance of linear momentum becomes

$$M_{\alpha\beta} \ddot{U}_{M\beta} = f_{M\alpha}^1 + f_{M\alpha}^2 + f_{M\alpha}^3 \tag{A9}$$

Based on the energy equation, the weak form of the conservation law of energy can be written as (cf. Eq. (97)) [7]

$$\begin{aligned}
 \int_V \left\{ \rho^\circ \gamma \frac{T + T^\circ}{T^\circ} \dot{T} + (T + T^\circ) \bar{A}_{KL} \dot{E}_{KL}^e \right. \\
 \left. - T_{KL}^{me} \dot{E}_{KL}^p - T_{KL}^d \dot{E}_{KL} + Q_{K,K} + P_K \dot{E}_K^* + M_K^* \dot{B}_K - J_K^* E_K^* - \rho^\circ h \right\} \delta T dV = 0 \tag{A10}
 \end{aligned}$$

The first term in the weak form becomes

$$\int_V \rho^\circ \gamma \frac{(T + T^\circ)}{T^\circ} \dot{T} \delta T dV = \dot{T}_\beta \delta T_\alpha \int_V \rho^\circ \gamma \frac{(N_\xi T_\xi + T^\circ)}{T^\circ} N_\alpha N_\beta dV \equiv \dot{T}_\beta \delta T_\alpha G_{\alpha\beta} \tag{A11}$$

The second term yields

$$\begin{aligned} & \int_V -(T + T^o) \bar{A}_{KL} \dot{E}_{KL}^e \delta T dV \\ &= \delta T_\alpha \int_V -(T + T^o) \bar{A}_{KL} \dot{E}_{KL}^e N_\alpha dV \equiv \delta T_\alpha q_\alpha^1 \end{aligned} \quad (A12)$$

The third term results

$$\int_V T_{KL}^{me} \dot{E}_{KL}^p \delta T dV = \delta T_\alpha \int_V T_{KL}^{me} \dot{E}_{KL}^p N_\alpha dV \equiv \delta T_\alpha q_\alpha^2 \quad (A13)$$

The fourth term is identified and derived as

$$\int_V T_{KL}^d \dot{E}_{KL} \delta T dV = \delta T_\alpha \int_V T_{KL}^d \dot{E}_{KL} N_\alpha dV \equiv \delta T_\alpha q_\alpha^3 \quad (A14)$$

The fifth term is identified and derived as

$$\begin{aligned} & \int_V \{-P_K \dot{E}_K^* - M_K^* \dot{B}_K + J_K^* E_K^*\} \delta T dV \\ &= \delta T_\alpha \int_V \{-P_K \dot{E}_K^* - M_K^* \dot{B}_K + J_K^* E_K^*\} N_\alpha dV \equiv \delta T_\alpha q_\alpha^4 \end{aligned} \quad (A15)$$

The sixth term can be derived as

$$\begin{aligned} & \int_V -Q_{K,K} \delta T dV = - \oint_S Q_K n_K \delta T dS + \int_V Q_K \delta T_{,K} dV \\ &= \delta T_\alpha \left\{ - \int_{S_q} \hat{Q} N_\alpha dS + \int_V Q_K N_{\alpha,K} dV \right\} \equiv \delta T_\alpha \{q_\alpha^5 + q_\alpha^6\} \end{aligned} \quad (A16)$$

where on the boundary surface,  $S_q$ ,  $Q_K n_K$  is specified as the heat flow  $Q$ , and  $n_K$  is the unit outward normal to the boundary surface.

The last term becomes

$$\int_V \rho^o h \delta T dV = \delta T_\alpha \int_V \rho^o h N_\alpha dV \equiv \delta T_\alpha q_\alpha^7 \quad (A17)$$

Now Eq. (A10) can be re-written as

$$\delta T_\alpha \{G_{\alpha\beta} \dot{T}_\beta - [q_\alpha^1 + q_\alpha^2 + q_\alpha^4 + q_\alpha^4 + q_\alpha^5 + q_\alpha^6 + q_\alpha^7]\} = 0 \quad (A18)$$

which implies the finite element equation for conservation law of energy becomes

$$G_{\alpha\beta} \dot{T}_\beta = q_\alpha^1 + q_\alpha^2 + q_\alpha^3 + q_\alpha^4 + q_\alpha^5 + q_\alpha^6 + q_\alpha^7 \quad (A19)$$

For scalar potential, the weak form of Eq. (99) is expressed as

$$\int_v \left\{ \frac{1}{c^2} \ddot{\phi} - (\phi_{,i})_{,i} - a \right\} \delta \phi dv = 0 \quad (A20)$$

Term by term one obtains

$$\int_v \frac{1}{c^2} \ddot{\phi} \delta \phi dv = \delta \phi_\alpha \ddot{\phi}_\beta \int_v \frac{1}{c^2} N_\beta N_\beta dv = \delta \phi_\alpha m_{\alpha\beta} \ddot{\phi}_\beta \quad (\text{A21})$$

$$\begin{aligned} \int_v -(\phi_{,i})_{,i} \delta \phi dv &= \int_v \{ -(\phi_{,i} \delta \phi)_{,i} + \phi_{,i} \delta \phi_{,i} \} dv \\ &= \delta \phi_\alpha \oint_s -\phi_{,i} n_i N_\alpha ds + \delta \phi_\alpha \phi_\beta \int_v N_{\alpha,i} N_{\beta,i} dv \\ &= \delta \phi_\alpha \int_{s_\xi} -\phi_{,i} n_i N_\alpha ds + \delta \phi_\alpha \phi_\beta \int_v N_{\alpha,i} N_{\beta,i} dv \\ &= -\delta \phi_\alpha \hat{\xi}_\alpha + \delta \phi_\alpha k_{\alpha\beta} \phi_\beta \end{aligned} \quad (\text{A22})$$

$$\int_v -a \delta \phi dv = \delta \phi_\alpha \int_v -a N_\alpha dv = -\delta \phi_\alpha \tilde{a}_\alpha \quad (\text{A23})$$

Therefore, one obtains

$$m_{\alpha\beta} \ddot{\phi}_\beta + k_{\alpha\beta} \phi_\beta = \hat{\xi}_\alpha + \tilde{a}_\alpha \quad (\text{A24})$$

where  $s_\xi$  is part of the enclosing surface of the volume  $v$  on which  $\phi_{,i} n_i$  is specified as  $\xi$ ;  $n_i$  is the unit outward normal to the enclosing surface; and

$$\begin{aligned} m_{\alpha\beta} &\equiv \int_v \frac{1}{c^2} N_\alpha N_\beta dv \\ k_{\alpha\beta} &\equiv \int_v N_{\alpha,i} N_{\beta,i} dv \\ \hat{\xi}_\alpha &\equiv \int_{s_\xi} \xi N_\alpha ds \equiv \int_{s_\xi} \phi_{,i} n_i N_\alpha ds \\ \tilde{a}_\alpha &= \int_v a N_\alpha dv \end{aligned} \quad (\text{A25})$$

For vector potential, the weak form of Eq. (100) is expressed as

$$\int_v \left\{ \frac{1}{c^2} \ddot{A}_k - \nabla^2 A_k - \tilde{C}_k \right\} \delta A_k dv = 0 \quad (\text{A26})$$

Term by term one obtains

$$\int_v \frac{1}{c^2} \frac{\partial^2 A_k}{\partial t^2} \delta A_k dv = \delta A_{k\alpha} \ddot{A}_{k\beta} \int_v \frac{1}{c^2} N_\alpha N_\beta dv = \delta A_{k\alpha} m_{\alpha\beta} \ddot{A}_{k\beta} \quad (\text{A27})$$

$$\int_v -A_{k,ii} \delta A_k dv = \int_v \{ -[A_{k,i} \delta A_k]_{,i} + A_{k,i} \delta A_{k,i} \} dv$$

$$\begin{aligned}
&= \delta A_{k\alpha} \oint_s -A_{k,i} n_i N_\alpha ds + \delta A_{k\alpha} A_{k\beta} \int_v N_{\alpha,i} N_{\beta,i} dv \\
&= \delta A_{k\alpha} \int_{s_c} -\tilde{A}_k N_\alpha ds + \delta A_{k\alpha} A_{k\beta} \int_v N_{\alpha,i} N_{\beta,i} dv \\
&\equiv \delta A_{k\alpha} \left\{ -\hat{A}_{k\alpha} + k_{\alpha\beta} A_{k\beta} \right\}
\end{aligned} \tag{A28}$$

$$\int_v -\tilde{C}_k \delta A_k dv = -\delta A_{k\alpha} \int_v \tilde{C}_k N_\alpha dv \equiv -\delta A_{k\alpha} \hat{C}_{k\alpha} \tag{A29}$$

Therefore, one obtains

$$m_{\alpha\beta} \ddot{A}_{k\beta} + k_{\alpha\beta} A_{k\beta} = \hat{A}_{k\alpha} + \hat{C}_{k\alpha} \tag{A30}$$

where  $s_c$  is part of the enclosing surface of the volume  $v$  on which  $A_{k,i} n_i$  is specified as  $\tilde{A}_k$ ; and

$$\begin{aligned}
\hat{A}_{k\alpha} &\equiv \int_{s_c} A_{k,i} n_i N_\alpha ds \equiv \int_{s_c} \tilde{A}_k N_\alpha ds \\
\hat{C}_{k\alpha} &\equiv \int_v \tilde{C}_k N_\alpha dv
\end{aligned} \tag{A31}$$

## References

1. Jackson JD. Classical electrodynamics. Hoboken, NJ, USA: John Wiley & Sons, Inc.; 1999.
2. De Groot SR, Suttrop LG. Foundations of electrodynamics. Amsterdam, The Netherlands: Elsevier; 1972.
3. Eringen AC. Mechanics of continua. 2nd ed. Melbourne, FL, USA: Krieger; 1980.
4. Eringen AC. Microcontinuum field theories I: Foundations and solids. New York, NY, USA: Springer; 1999. doi:10.1007/978-1-4612-0555-5.
5. Eringen AC, Maugin GA. Electrodynamics of continua I: Foundations and solid media. New York, NY, USA: Springer-Verlag; 1990. doi:10.1007/978-1-4612-3236-0.
6. Eringen AC, Maugin GA. Electrodynamics of continua II: Fluids and complex media. New York, NY, USA: Springer; 1990. doi:10.1007/978-1-4612-3236-0.
7. Lee JD, Li J. Advanced continuum theories and finite element analyses. Singapore: World Scientific; 2019. doi:10.1142/11312.
8. Eringen AC. Nonlocal continuum field theories. New York, NY, USA: Springer; 2002.
9. Coleman BD, Noll W. The thermodynamics of elastic materials with heat conduction and viscosity. Arch Ration Mech Anal. 1963;13(1):167–78. doi:10.1007/BF01262690.
10. Casey J. On elastic-thermo-plastic materials at finite deformations. Int J Plast. 1998;14(1–3):173–91. doi:10.1016/S0749-6419(97)00047-8.
11. Green AE, Naghdi PM. A general theory of an elastic-plastic continuum. Arch Ration Mech Anal. 1965;18(4):251–81. doi:10.1007/BF00251666.
12. Onsager L. Reciprocal relations in irreversible processes I. Phys Rev. 1931;37(4):405–26. doi:10.1103/physrev.37.405.
13. Onsager L. Reciprocal relations in irreversible processes II. Phys Rev. 1931;38(12):2265–79. doi:10.1103/physrev.38.2265.
14. Li J, Lee JD. Molecular simulations and multiphysics nanoscale coupling. New York, NY, USA: CRC Press; 2026.
15. Gong Z, Zhang Y, Pan E, Zhang C. Three-dimensional general magneto-electro-elastic finite element model for multiphysics nonlinear analysis of layered composites. Appl Math Mech Engl Ed. 2023;44(1):53–72. doi:10.1007/s10483-023-2943-8.
16. Li X, Yang H, Zhu P, Li X, Yuan X. The coupling multiscale finite element method for transient responses of heterogeneous magneto-electro-elastic structures in thermal environment. J Mech. 2025;41(3):355–76. doi:10.1093/jom/ufaf028.

17. Wang S, Tang Y, Yong H, Zhou Y. A coupled electromagnetic-mechanical model and contact behavior of the superconducting coils. *Appl Math Model.* 2024;133(1):491–511. doi:10.1016/j.apm.2024.05.042.
18. Kanan A, Polukhov E, Keip MA, Dorfmann L, Kaliske M. Computational material stability analysis in finite thermo-electro-mechanics. *Mech Res Commun.* 2022;121:103867. doi:10.1016/j.mechrescom.2022.103867.